Simulation of the cavitating flow in a model oil hydraulic spool valve using different model approaches

peer reviewed

Dipl.-Ing. Michel Schümichen, Dr.-Ing. Frank Rüdiger, Professor Dr.-Ing. habil. Jochen Fröhlich

Institut für Strömungsmechanik (ISM), Technische Universität Dresden, George-Bähr-Straße 3c, 01069 Dresden, E-Mail: michel.schuemichen@tu-dresden.de

Professor Dr.-Ing. Jürgen Weber

Institut für Fluidtechnik (IFD), Technische Universität Dresden, Helmholtzstrasse 7a, 01069 Dresden, E-Mail: mailbox@ifd.mw.tu-dresden.de

Abstract

The contribution compares results of Large Eddy Simulations of the cavitating flow in a model oil hydraulic spool valve using an Euler-Euler and a one-way coupled Euler-Lagrange model. The impact of the choice of the empirical constants in the Kunz cavitation model is demonstrated. Provided these are chosen appropriately the approach can yield reasonable agreement with the corresponding experiment. The one-way Euler-Lagrange model yields less agreement. It is demonstrated that this is due to the lack of realistic volumetric coupling, rarely accounted for in this type of method. First results of such an algorithm are presented featuring substantially more realism.

KEYWORDS: Cavitation, oil hydraulics, spool valve, Large-Eddy Simulation, Euler-Lagrange model, Euler-Euler model

1. Introduction

Cavitation is a physical phenomenon that occurs in liquid flows when the liquid pressure falls below a critical pressure, generally of the order of the vapour pressure p_v /1/. As a consequence, vapour bubbles are formed and convected by the flow. They collapse in regions where the pressure rises again above the critical pressure. Cavitation denotes the whole process of vaporization, convection and collapse and occurs in many industrial applications such as valves, pumps, hydrofoils, chemical homogenizers and industrial cleaning. Additionally, diffusion of dissolved non-condensable gas from the liquid to the cavitation bubble can occur, the so-called gas cavitation which, however, is not addressed here. In many cases cavitation is an undesired phenomenon since it is often associated with a substantial loss of efficiency,

as well as noise and wear. This also holds for oil hydraulic spool valves considered here. Although it is not possible to avoid cavitation in such components, it is, however, desirable to make statements about the cavitation intensity in an early design phase with the purpose to reduce it to a minimum. Due to the high effort needed for experiments the accurate prediction of cavitation by simulations becomes more and more important for the design of oil hydraulic devices. Common numerical cavitation models can be divided into three different approaches: a) models based on an equation of state for the homogenized fluid /2/, b) Euler-Euler models/3/ and c) Euler-Lagrange models/4/. The second approach considers the multiphase flow only in a statistical sense based on effective material properties of the liquid-vapour mixture and is state of the art in industrial applications and commercial flow solvers. In contrast, the Euler-Lagrange model describes the vapour phase by discrete spherical bubbles treated in a Lagrangian manner thus offering new possibilities for the fundamental understanding of cavitation /5/. The representation of microbubbles as cavitation nuclei allows a safe modelling of cavitation inception, for instance. Properties of nuclei, such as the nuclei size spectrum and hence the liquid quality, can be taken into account directly with such a model. Furthermore, the Euler-Lagrange model is free of numerical diffusion for the dispersed vapour phase. It also allows direct modelling of gas cavitation which plays an important role for oil hydraulic flow. Moreover, it also offers very detailed temporal information for individual bubbles that can be used to calculate other physical properties such as erosion intensity or sound pressure level. Besides that, another advantage of the Euler-Lagrange approach is that it does not contain empirical constants, except coefficients for the momentum transfer, such as the drag coefficient, which are general and not cavitation specific, though. Hence, no calibration of the model for a specific configuration is necessary, as it is in the case of models based on the Euler-Euler approach. The present contribution compares results of Large Eddy Simulation (LES) of the cavitating flow in a model oil hydraulic spool valve using an Euler-Euler model and an own one-way coupled Euler-Lagrange model. The aim of this contribution is to compare the capabilities of the Euler-Euler approach and the Euler-Lagrange approach for the simulation of cavitation. Using the results to optimize the valve geometry will be part of future work.

2. Numerical modelling of cavitating flows

In the Euler-Euler model the multiphase flow is described as a liquid-vapour mixture where the effective material properties linearly depend on the liquid volume fraction α_1. For the density ρ, this ready

$$\rho = \rho_l \alpha_l + \rho_v (1-\alpha_l) \quad . \tag{1}$$

The pure phases are treated incompressible with constant densities ρ_l and ρ_v for the liquid and the vapour phase, respectively. The mixture is governed by the compressible Navier-Stokes equations for a Newtonian fluid

$$\nabla \cdot \underline{u} = \left(1 - \frac{\rho_l}{\rho_v}\right) S \quad , \frac{\partial(\rho \underline{u})}{\partial t} + \nabla \cdot \left(\rho \underline{u}\underline{u}\right) = -\nabla p + \nabla \cdot \underline{\underline{\tau}} \tag{2}$$

together with a transport equation for the liquid volume fraction

$$\frac{\partial \alpha_l}{\partial t} + \nabla \cdot \left(\alpha_l \underline{u}\right) = \mathrm{S} \tag{3}$$

to close the equation system. Here, $\underline{u}$ is the velocity vector, p the pressure, $\underline{\underline{\tau}} = \mu\left(\nabla \underline{u} + \left(\nabla \underline{u}\right)^{\mathrm{T}} - 2/3 \nabla \cdot \underline{u}\, \underline{\underline{I}}\right)$ the shear stress tensor and μ the dynamic viscosity. Note that a non-conservative form of the continuity equation is used that expresses the divergence of the velocity field in terms of the source term in (3) and is very important for the stability of the flow solver. The source term S models condensation and evaporation and depends on the cavitation model used. Here, the Kunz model /3/ without accounting for non-condensable gases is applied

$$S = \frac{\rho_v}{\rho_l} \frac{C_{\mathrm{evap}} \min(0, p - p_v)}{\rho_l / 2 u_{\mathrm{in}}^2 \, t_{\mathrm{in}}} + \frac{\rho_v}{\rho_l} \frac{C_{\mathrm{cond}} \alpha_l^2 (1-\alpha_l)}{t_{\mathrm{in}}} \quad , \tag{4}$$

where p_v denotes the vapour pressure, u_∞ and t_∞ are characteristic velocity and time related to the bulk inflow. The necessity to calibrate the empirical constants C_{evap} and C_{cond} is a major drawback of the model as this needs to be done for each specific configuration.

With the Euler-Lagrange approach the two phases are described in different frames of reference. The continuous liquid phase, index l, is represented in an Eulerian frame employing the incompressible Navier-Stokes equations

$$\nabla \cdot \underline{u}_l = 0 \quad , \frac{\partial \underline{u}_l}{\partial t} + \nabla \cdot \left(\underline{u}_l \underline{u}_l\right) = -\frac{1}{\rho_l} \nabla p_l + \frac{1}{\rho_l} \nabla \cdot \underline{\underline{\tau}} \quad . \tag{5}$$

The trajectories of the discrete bubbles are described in the Lagrangian frame by Newton's equations of motion

$$\frac{\mathrm{d}\underline{x}_\mathrm{b}}{\mathrm{d}t} = \underline{u}_\mathrm{b} \quad , m_\mathrm{b} \frac{\mathrm{d}\underline{u}_\mathrm{b}}{\mathrm{d}t} = -\frac{1}{2} C_\mathrm{D} \rho_\mathrm{l} \pi r_\mathrm{b}^2 |\underline{u}_\mathrm{b} - \underline{u}_\mathrm{l}| (\underline{u}_\mathrm{b} - \underline{u}_\mathrm{l}) \quad , \tag{6}$$

where $\underline{x}_\mathrm{b}$ denotes the bubble coordinate vector, $\underline{u}_\mathrm{b}$ the bubble velocity vector, $m_\mathrm{b} = \rho_\mathrm{b}(4/3)\pi r_\mathrm{b}^3$ the bubble mass, r_b the bubble radius, and ρ_b the bubble density. The drag coefficient C_D is used as given in /8/. Other interfacial forces such as lift force or the force due to the far field pressure gradient are neglected in the present study.

The variation of bubble volume is modelled by the Rayleigh-Plesset equation /9/

$$\rho_\mathrm{l} \left(r_\mathrm{b} \frac{\mathrm{d}^2 r_\mathrm{b}}{\mathrm{d}t^2} + \frac{2}{3} \left(\frac{\mathrm{d}r_\mathrm{b}}{\mathrm{d}t} \right)^2 \right) = p_\mathrm{v} + p_\mathrm{g0} \left(\frac{r_\mathrm{b0}}{r_\mathrm{b}} \right)^{3n} - p_\mathrm{l} - \frac{2\sigma}{r_\mathrm{b}} - \frac{4\mu_\mathrm{l}}{r_\mathrm{b}} \frac{\mathrm{d}r_\mathrm{b}}{\mathrm{d}t} \, , \tag{7}$$

where σ is the surface tension coefficient, p_g0 the initial gas pressure, and r_b0 the initial bubble radius. The second term on the right-hand side of (7) is the partial pressure due contaminant gas in the bubble which expands or contracts according to the polytropic index n. Bubble expansion is modelled as isothermal and compression as adiabatic. The initial gas pressure is obtained from the condition that the bubble needs to be at equilibrium in the initial state.

3. Computational setup and testcase

The models described in the previous sections were implemented in the in-house finite-volume code LESOCC2 /10/. Details can be found in /11,12/. In the present contribution the cavitating flow in a model of a typical hydraulic spool valve is simulated (**Figure 1**, left). It was developed and experimentally investigated at IFD, Dresden, and consists of a supply channel followed by an orifice with 0,95mm gap width and a downstream valve chamber ending in a discharge channel. To ensure good optical access the model has a plain geometry. The velocity field and bubble distribution were obtained at the same instant in time via combined PIV/LIV/Shadowgraphy /5/. The computational domain was chosen as shown in **Figure 1**, right. The spool valve is operated with HLP46 hydraulic oil at a working temperature of 41.5 °C. The operating point considered here is characterized by a pressure loss of $\Delta p = 10$ bar which corresponds to a flow rate of 10 l/min. The pressure at the outlet is 4.7 bar.

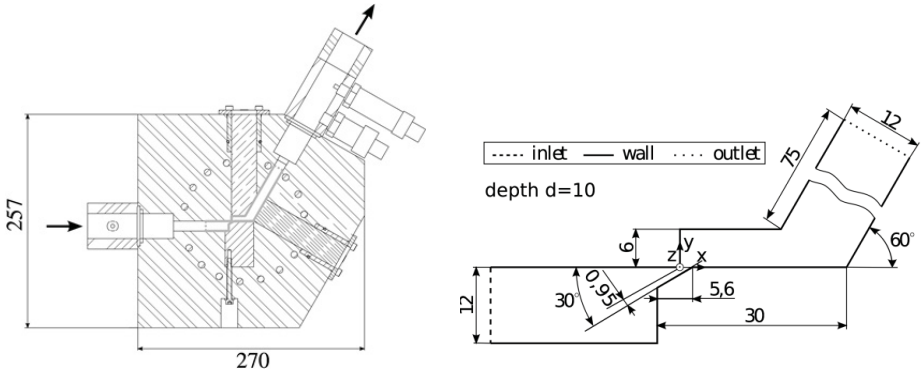

Figure 1: Technical drawing of the experimental setup (left) and the computational domain (right). Distances are in mm.

The flow was simulated by LES using a mesh with 10.3 million cells. Due to the high kinematic viscosity of the hydraulic oil the Reynolds number based on the bulk inflow velocity and the height of the supply channel is $\mathrm{Re}_{\mathrm{in}} = 856$ which is very untypical for LES. Indeed, the turbulence of the flow is very weak and the simulation effectively is a Direct Numerical Simulation, apart from the wall modelling as shown in /12/. The WALE model /13/ was used as subgrid-scale model with the model constant $C_{\mathrm{W}} = 0.21$, but due to the low Reynolds number had a little impact. The vapour pressure was assumed to be 0.2 bar. In the Euler-Lagrange model cavitation nuclei were continuously supplied at the inlet with an initial bubble radius r_{b0} of $5\,\mu\mathrm{m}$. Coalescence and break up of bubbles are not considered here and will be part of future work. The vapour phase consists of oil vapour and air where the material properties of the mixture are assumed to be that of air at standard conditions.

4. Results

As a reference, the incompressible single phase flow is examined first. In **Figure 2** the averaged velocity field in the centre of the valve chamber is shown together with the instantaneous velocity field for an arbitrarily chosen instant of time.

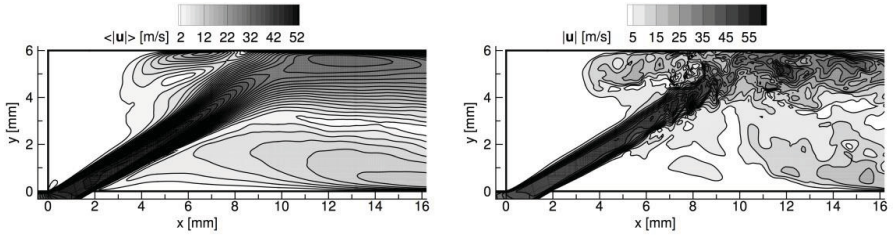

Figure 2: Simulation of non-cavitating flow in the centre plane. Left: average velocity magnitude, right: instantaneous velocity magnitude.

As can be seen the flow through the small orifice leads to the development of an unsteady internal jet in the valve chamber. It is laminar in the region of the orifice and remains laminar over a substantial distance until it becomes unstable at about one third of the chamber height. Disturbances in the shear layer of the jet grow leading to the development of Kelvin-Helmholtz (KH) vortices on each side of the jet. Transition takes place before the jet hits the upper part of the chamber. As shown in /11/, the occurrence of cavitation in the spool valve investigated here cannot be explained by the mean flow features and is only a result of the unsteady nature of the flow. The pressure drops significantly under the critical pressure at the centres of the KH vortices in the shear layers. These unsteady pressure minima are mainly responsible for the initial growth of the cavitation nuclei into large cavitation bubbles, while turbulent pressure fluctuations affect the subsequent behaviour of the bubbles.

First, the Kunz model was applied to simulate the cavitating flow in the context of an Euler-Euler model. Four different sets for the empirical constants C_{evap} and C_{cond} were used: 1) 100 for both of them as in /3/, 2) 4100 and 455 as found to be the optimum for the flow investigated in /6/, 3) 9e5 and 3e4 /7/ and 4) 1000 and 10, respectively. The comparison of the instantaneous fields is not reasonable for unsteady, turbulent flows, so that the time-averaged vapour volume fraction is shown in **Figure 3**. It can be compared to the experimental result in **Figure 4**, left.

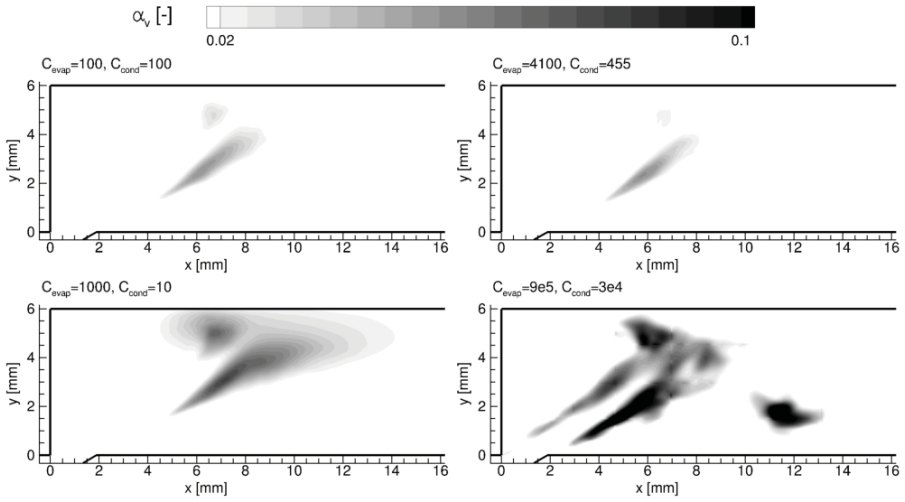

Figure 3: Averaged vapour volume fraction of the cavitating flow in simulations with Euler-Euler Kunz model for different sets of empirical constants.

Obviously, the amount of vapour as well as the vapour distribution is strongly affected by the choice of the model constants. Of the cases considered, the best agreement with the experiment is found for case 1 (top left in Figure 3).The result in this case is obtained by averaging over all cavitation events in time and hence not normalized. Local maxima can be observed in the shear layers of the jet for both the experiment as well as the simulations. In the experiment the bubble grows earlier than in the simulations and also collapse earlier.

The same result obtained with the Euler-Lagrange method is depicted in Figure 4, right, and typical instantaneous bubble distributions from experiment and the Euler-Lagrange simulation are shown in **Figure 5**. The void fraction distribution looks somewhat similar to case 4 with the Euler-Euler-Kunz model shown in Figure 3, bottom left, with a higher bubble concentration is observed in the upper part of the valve chamber, though. In both, experiment and simulation, relatively few but large bubbles are observed, with diameter of about 20% of the height of the valve chamber. Occasionally, even larger bubbles of up to twice of this diameter are observed in the simulation. This, however, is an artefact resulting from the neglected volumetric coupling and will be significantly improved when the effect is accounted for. This issue is addressed in the next section.

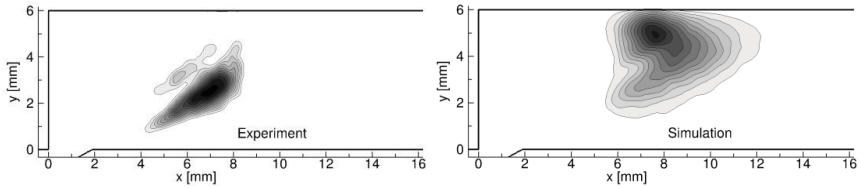

Figure 4: Qualitative comparison of cavitation bubble distribution by averaging of gray-scale plots. Left: Experiment, right: simulation with Euler-Lagrange model.

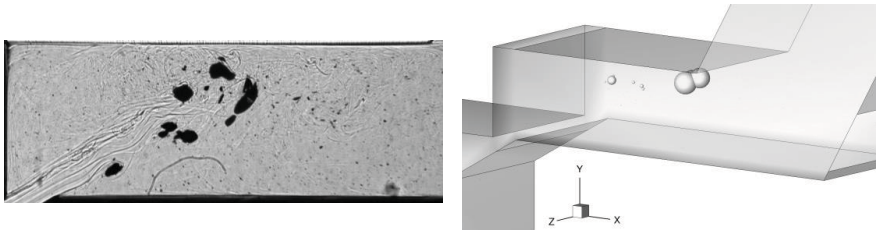

Figure 5: Snapshot of bubble distribution for an arbitrary instant in time. Left: Experiment, right: Euler-Lagrange model.

5. Influence of volumetric coupling in the Euler-Lagrange approach

As mentioned in the previous section neglecting in the Euler-Lagrange model the displacement of liquid due to variations of the bubble volume, the so-called volumetric coupling, leads to an overestimation of cavitation in the simulation compared to experimental observations. Unfortunately, the development of a robust solution algorithm accounting for volumetric coupling is very challenging due to the strong pressure-velocity-density coupling and the treatment of the different phases in different frames of reference. To the best of the author's knowledge the only method for unsteady simulations of cavitation with an Euler-Lagrange model that accounts for volumetric coupling was proposed by Shams et al. /4/ employing a Low-Mach number pressure-based algorithm.

To investigate the influence of the volumetric coupling, simulations of a single cavitating bubble in a nozzle flow were conducted in the present project. **Figure 6** shows the temporal history of the bubble radius of an initial cavitation nucleus without and with consideration of volumetric coupling (label 1-way and 2-way, respectively).

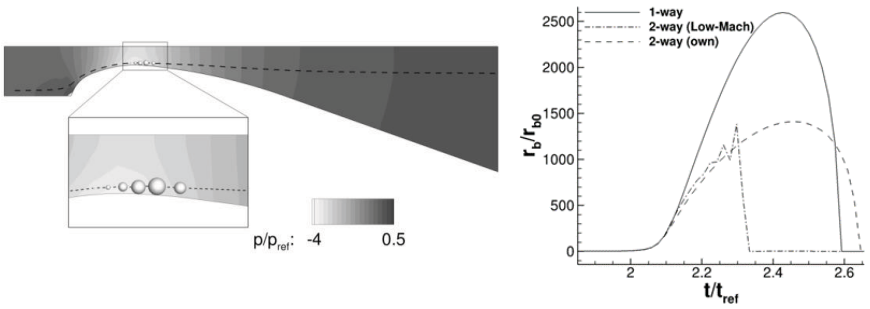

Figure 6: Evolution of a cavitating bubble in a nozzle flow. Left: Configuration and trajectory of the bubble with representation of the bubble at several instants of time for the case without volumetric coupling. The contour plot shows the pressure field. Right: Temporal Evolution of the bubble radius without volumetric coupling (label 1-way), with volumetric coupling according to /4/ (2-way (Low-Mach)), as well as with stable solver developed by the authors (2-way (own)).

The pressure rises in the vicinity of a growing bubble due to liquid displacement leading to an obvious decrease of the bubble growth compared to the case without volumetric coupling (label 1-way).The Low-Mach number solver proposed in /4/ was implemented as well, but it leads to an early unphysical bubble collapse with a subsequent bubble rebound. This behaviour originates from the insufficient coupling between the flow solver and the bubble dynamics for large rates of bubble growth and hence yields an unstable simulation. From a principle point of view, a solution algorithm based on a Low-Mach number approach cannot be promising since it is based on the independence of pressure and density and seems to be applicable only for very small bubble growth rates. Hence, this method is found unsuitable for the simulations of cavitation in the spool valve under the operating conditions investigated here. In order to cope with this issue, a new stable solution method was developed for arbitrary large bubble growth rates (label 2-way (own) in Figure 6). As can be seen the bubble behaviour seems physically reasonable and the bubble life time as well as the maximum bubble radius are both affected by the volumetric coupling.

6. Conclusions

The cavitating flow in a model hydraulic spool valve was simulated by means of Large-Eddy Simulation in conjunction with an Euler-Euler and a one-way coupled Euler-Lagrange model. The result obtained by the Euler-Euler Kunz model strongly depends on the choice of the empirical constants. Both approaches can lead to similar results

that are in reasonable agreement with experiments in terms of bubble locations and bubble size. For the Euler-Lagrange model the importance of the volumetric coupling for the bubble dynamics, disregarded in other methods, was demonstrated. Work in this direction is under way.

7. Acknowledgements

The present work is funded by the German Research Foundation (DFG) via the project FR 1593/7-1. We thank the Centre for Information Services and High Performance Computing (ZIH) at TU Dresden for allocation of computer time.

8. References

/1/ Heller, W., Hydrodynamische Effekte unter besonderer Berücksichtigung der Wasserqualität und ihre Messverfahren. Habilitationsschrift, InstitutfürStrömungsmechanik, TechnischeUniversität Dresden, 2005.

/2/ Egerer, C. P., Hickel, S., Schmidt, S. J., Adams, N. A., Large-eddy simulation of turbulent cavitating flow in a micro channel. Physics of Fluids 26:085102, 2014.

/3/ Kunz, R. F., Boger, D. A., Stinebring, D. R., Chyczewski, T. S., Lindau, J. W., Gibeling, H. J., Venkateswaran, S., Govindan, T. R., A preconditioned Navier–Stokes method for two-phase flows with application to cavitation prediction. Computers & Fluids 29(8):849-875, 2000.

/4/ Shams, E., Finn, J., Apte, S. V., A numerical scheme for Euler–Lagrange simulation of bubbly flows in complex systems. International Journal for Numerical Methods in Fluids 67(12):1865–1898, 2011.

/5/ Müller, L., Helduser, S., Weber, J., Schümichen, M., Rüdiger, F., Fröhlich, J., Groß, T., Ludwig, G., Pelz, P., Messverfahren und numerische Modellierung von Kavitation in einem ölhydraulischen Ventil. Ölhydraulik und Pneumatik 57(2):20-26, 2013.

/6/ Morgut, M., Nobile, E., Bilus, I., Comparison of mass transfer models for the numerical prediction of sheet cavitation around a hydrofoil. International Journal of Multiphase Flow 37(6):620-626, 2011.

/7/ Senocak, I. and Shyy, W, Interfacial dynamics-based modelling of turbulent cavitating flows, Part-1: Model development and steady-state computations.

International Journal of Numerical Methods in Fluids 44:975-995, 2004.

/8/ Haberman, W. L., Morton, R. K., An experimental investigation of the drag and shape of air bubbles rising in various liquids. DTMB Report No. 802, 1953.

/9/ Brennen, C. E., Cavitation and Bubble Dynamics. Oxford University Press New York, 1995.

/10/ Hinterberger, C., Fröhlich, J., Rodi, W., 2D and 3D turbulent fluctuations in open channel flow with studied by Large Eddy Simulation. Flow Turbulence and Combustion 80:225-253, 2008.

/11/ Schümichen, M., Rüdiger, F., Weber, J., Fröhlich, J., One-way coupled Euler-Lagrange simulation of the cavitatingflow in a model hydraulic spool valve. Strömungstechnische Tagung 2014, Schriftenreihe aus dem Institut für Strömungsmechanik, Band 10, TUDpress, Dresden, 2014.

/12/ Schümichen, M., Joppa, M., Rüdiger, F., Fröhlich, J., Müller, L., Weber, J., Helduser, S., Simulation of the turbulent flow in a model hydraulic spool valve. Proceedings in Applied Mathematics and Mechanics 13:303-304, 2013.

/13/ Nicoud, F., Ducros, F., Subgrid-scale stress modelling based on the square of the velocity gradient tensor. Flow, Turbulence and Combustion 62(3):183-200, 1999.

9. Nomenclature

α	Volume fraction	-
C_{cond}	Empirical model constant in the Kunz model	-
C_{D}	Drag coefficient	-
C_{evap}	Empirical model constant in the Kunz model	-
C_{W}	Model constant of the WALE model	-
Δp	Pressure loss	Pa
$\underline{\underline{I}}$	Identity matrix	-

κ	Adiabatic index	-
m	mass	kg
μ	Dynamic viscosity	Pa s
n	Polytropic index	-
p	Pressure	Pa
p_{g0}	Initial gas pressure	Pa
r	Radius	m
$\mathrm{Re}_{\mathrm{in}}$	Reynolds number related to the bulk inflow	-
ρ	Density	kg/m^3
S	Source term	1/s
σ	Surface tension coefficient	N/m
t	time	s
$\underline{\underline{\tau}}$	Shear stress tensor	Pa
u	Velocity magnitude	m/s
$\underline{u}$	Velocity vector	m/s
$\underline{x}$	Spatial coordinate vector	m

Subscripts (denoted for an arbitrary quantity ϕ)

ϕ_{b}	Physical quantity related to a discrete bubble
ϕ_{b0}	Physical quantity related to the initial state of a discrete bubble
ϕ_{l}	Physical quantity related to the liquid phase
ϕ_{v}	Physical quantity related to the vapour phase